Thermal behaviour of iron arsenides under non-oxidising conditions[†]

Ainur Seitkan,[*,‡] Giulio I. Lampronti,[*,¶] Remo N. Widmer,[¶] Nicola P.M. Casati,[§] and Simon A.T. Redfern[*,‖]

‡*School of Natural Sciences, Astana International University, Nur-Sultan, Kazakhstan*
¶*Department of Earth Sciences, University of Cambridge, Downing Street, Cambridge, CB2 3EQ, UK*
§*Swiss Light Source, Paul Scherrer Institute, Villigen, Switzerland*
‖*Asian School of the Environment, Nanyang Technological University, 639798 Singapore*

E-mail: seitkanainur.77@mail.ru; gil21@cam.ac.uk; Simon.Redfern@ntu.edu.sg

Abstract

Fe_2As has been studied *in-situ* by synchrotron PXRD over the range of temperatures 25-850 °C and under neutral atmosphere to understand its thermal behaviour, which is potentially important for gold extraction. For the first time, incongruent high temperature reactions of Fe_2As are observed as it breaks down and the existence of a previously-undiscovered high-temperature FeAs phase with NiAs-type structure has been determined experimentally. No evidence has been found for existence of the high-temperature phase Fe_3As_2. Hence, the previously published phase diagram for the Fe-As system has to be modified accordingly.

[†]Thermal behaviour of iron arsenides under non-oxidising conditions

Introduction

Due to resource depletion of easily-processed non-ferrous and precious metals, metallurgical processing is increasingly moving towards refractory ores and concentrates with high arsenic (As) content. In this regard, the problem of As removal, and countering the problems it adds to the technological process of obtaining end product metals, becomes absolutely critical.

Iron arsenides may be the key to extraction of gold from double refractory gold-arsenic-bearing carbonaceous ores, where gold is not extractable without significant ecological contamination from the associated arsenopyrite mineralisation. By processing under reducing atmospheres in the presence of an iron-rich slag, certain proposed direct reductive melting (DRM) processes lock As into iron arsenide phases[1]. The effectiveness of As removal from arsenic-bearing gold concentrates is directly associated with the decomposition of such iron arsenides. Hence, development of the DRM process demands an improved fundamental understanding of the thermal behaviour of the iron-arsenic phases of interest, especially the main constituent Fe_2As diiron arsenide. There is no information on the thermal behavior of diiron arsenide in reducing and inert atmospheres, which are those characteristic of the conditions of the DRM process.

The Fe-As system

Initial interest in the Fe-As system originated from the need to minimise the negative ecological and environmental impacts of As resulting from metallurgical processing, since it often accompanies non-ferrous and precious metals in sulfidic ores. The application of As-containing compounds in electronic devices, and the discovery of their thermoelectric and superconducting properties fuelled further interest in the Fe-As system.

The Fe-As system has been extensively reviewed by Okamoto[2]. The phase diagram of the Fe-As system is shown in Figure 1. The phases are: $\alpha-$As, $FeAs_2$, FeAs, Fe_3As_2, Fe_2As, $\alpha-$Fe and $\gamma-$Fe. The existence of a high-temperature Fe_3As_2 phase was previously

postulated, but never confirmed experimentally[2].
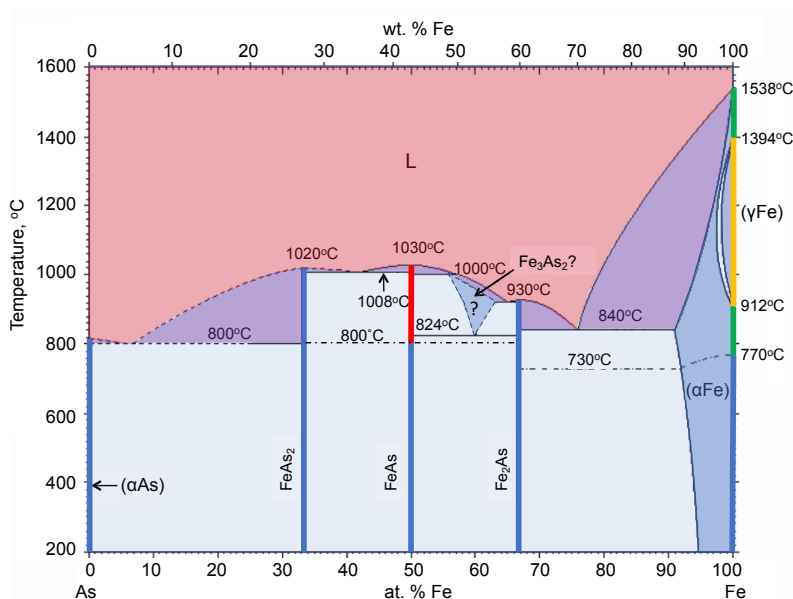
Figure 1: Phase diagram of the Fe-As system adapted from Okamoto[2]. Line phases are shown dark blue at room temperature and alternatively colored where polymorphs occur at high temperature. The postulated stability field of the Fe_3As_2 phase is indicated.

The known minerals occurring in this system are loellingite ($FeAs_2$) and westerveldite ($FeAs$). Crystallographic data of previously-reported iron arsenides stable at room temperature are given in Table 1.

Table 1: Crystallographic data of iron arsenides

Phase	Space group	Structure type	Reference
Iron arsenide (2/1) Fe_2As	$P4/nmm$	Cu_2Sb	[3]
Iron (III) arsenide FeAs	$Pnma$	MnP	[4]
Iron diarsenide $FeAs_2$	$Pnnm$	FeS_2	[5]

The congruent melting points of $FeAs_2$, FeAs, and Fe_2As are 1020 °C[6], 1030 °C[7], and 919 °C[7] (or 930 °C[8]), respectively. A high-temperature study of the stoichiometric FeAs

phase showed that the MnP type crystal structure remains virtually unchanged up to 1300 K (1027°C)[9]. A high-pressure X-ray study of an FeAs single crystal did not reveal any deviation from the MnP structure throughout the applied pressure range[10].

Studies on the thermal behavior of iron arsenides

Previous studies of the thermal behavior of iron arsenides under various atmospheres had two principal aims: first, a better understanding of de-arsenication mechanisms of refractory gold-arsenic-bearing ores and concentrates, and the optimisation of gold recovery technologies, and second, attempts to improve the commercial production of high-purity As in vacuum. Information on the thermal behavior of iron arsenides in reducing and neutral atmospheres is very limited. Earlier studies on the thermal behavior of natural loellingite ($FeAs_2$) at 450-800 °C and one atmospheric pressure reported that loellingite decomposes with the release of As, and formation of FeAs[11]. The thermal behavior of synthetic iron arsenides under vacuum (<0.0106 kPa) was studied by Tkach et al., 1977[12]. Heating of the 0.074-0.14 mm grain sized material at a rate of $10° \, min^{-1}$ indicated the following mechanism of decomposition:

$$FeAs_2 \xrightarrow{>700°C} FeAs \xrightarrow{>900°C} Fe_2As. \tag{1}$$

In contrast, Isabayev et al., 1986[13] observed only one endothermic effect at 940 °C from the differential thermal analysis (DTA) curve of a synthetic iron diarsenide heated under a helium atmosphere.

Thorough investigation of thermal behaviour of iron arsenides $FeAs_2$ and FeAs in vacuum has been conducted previously[14]. Arsenides were prepared by sintering a mixture of metallic arsenic and iron in evacuated quartz ampoules. The resulting synthetic iron diarsenide, according to the mineralogical and X-ray structure analysis, contained about 10% FeAs and corresponded to a formula unit of $Fe_{1.05}As_{1.95}$. The synthesized iron monoarsenide contained about 2% $FeAs_2$. An exothermic peak at 320 to 350 °C and an endothermic effect at 650-

640 °C, accompanied by loss in weight, was observed on the DTA analysis of $FeAs_2$. The endothermic effect was attributed to the decomposition of iron diarsenide. The DTA study of FeAs showed an exothermic peak at 340-360 °C and an endothermic peak at 630-650 °C, accompanied by a slight decrease of mass. A noticeable loss of weight was observed at 820-830 °C. Powder X-ray diffraction (PXRD) and electron probe micro-analysis (EPMA) of the solid products of monoarsenide decomposition at temperatures above 800 °C revealed the presence of Fe_2As. Diarsenide dissociation was investigated by *in-situ* high temperature X-ray diffraction when heating in a vacuum of 0.1 Pa over a temperature range of 25-900 °C. X-ray patterns were taken every 50 to 100 °C. It was found that $FeAs_2$ decomposition commences at 400 °C and ends at 600 °C with formation of FeAs. Visible decomposition of FeAs was observed at 650 °C and was completed above 800 °C with the formation of diiron arsenide Fe_2As as a solid-phase. The authors came to the conclusion that the thermal dissociation of iron diarsenide under vacuum has a stepwise nature:

$$FeAs_2 \xrightarrow{510\text{-}690°C} FeAs_{1.5} + \frac{1}{8}As_4(g) \tag{2}$$

$$FeAs_{1.5} \xrightarrow{690\text{-}805°C} FeAs + \frac{1}{8}As_4(g) \tag{3}$$

$$FeAs \xrightarrow{805\text{-}1200°C} FeAs_{0.5} + \frac{1}{8}As_4(g) \tag{4}$$

$$FeAs_{0.5} \xrightarrow{>1200°C} \frac{1}{2}Fe_2As + \frac{1}{2}Fe \tag{5}$$
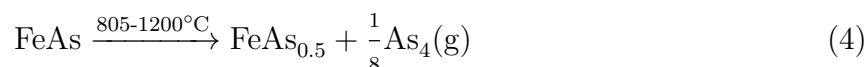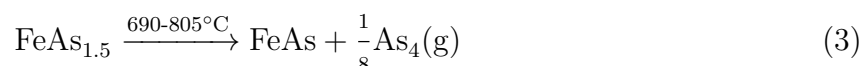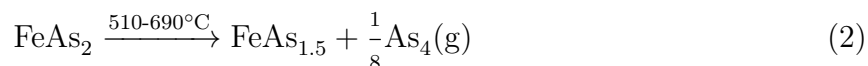
Thus, As is present in the form of diiron arsenide in the residues of thermal decomposition of arsenopyrite and iron arsenides at temperatures above 900-1200 °C, heated in inert atmosphere or vacuum [12,14,15].

Thus far, however, no single study has reported on the thermal behaviour of diiron arsenide. Hence data on the thermal behaviour of Fe_2As in neutral and reducing atmospheres, which are characteristic of the conditions of any proposed DRM process, are essential. The aim of this study is to fill this gap in our understanding, and study the thermal behaviour of diiron arsenide by conducting *in situ* high-temperature synchrotron XRD of diiron arsenide.

This is the first high-temperature structural study of Fe_2As.

Experimental Methods

In situ high-temperature powder X-ray diffraction was conducted at the Materials Science Beamline of the Swiss Light Source (SLS) of the Paul Scherrer Institute (PSI), Switzerland)[16]. This diffractometer yielded an exceptionally high angular resolution and data quality: despite the small binning step (0.0036°) some of the sharpest peaks appeared undersampled, with less than five data points above the half maximum (inset in Figure 3). This complicated the the peak fitting somewhat. Nevertheless, the data quality allowed for high precision cell parameters to be determined and the identification of unexpected high-temperature phases including a new previously unreported high temperature phase of FeAs. The experiments were performed at the powder diffraction station of the X04SA using monochromatic radiation ($\lambda = 0.56502$ Å). The starting $FeAs_2$ samples were ground using a mortar and a pestle manually, sieved through a 75 µm sieve, mixed, and weighed. The preparation of the samples required the use of a glovebag under nitrogen to prevent oxidation of As. The experiments simulated the conditions of the DRM process. Samples of 99.5% Fe_2As (commercial, Alfa Aesar) were thus loaded under nitrogen into quartz capillaries with internal diameter of 0.1 mm and sealed. Phase changes were monitored throughout the heating and cooling profile by *in situ* PXRD.

Raw diffraction data were processed and merged using in-house software. The structural changes associated with limits of stability were determined by Rietveld analysis. Parametric Rietveld refinements were performed using Topas V4.1[17]. Parameters of the Mythen detector position and intensity correction model, the specimen displacement, the divergence slit, and the instrumental contribution for peak broadening using the Gaussian parameters of a Pseudo-Voigt function were refined globally against the entirety of all datasets. This lowers the corresponding estimated standard deviations because of the larger number of observations

and minimises the overall number of free parameters. Simultaneously, background, phase compositions, unit cell dimensions, and microstrain related Lorentzian peak broadening were refined individually for all phases at all temperatures. March-Dollase preferred-orientation corrections were applied to the (0 0 1) plane of Fe_2As. The background was modelled with a Chebyshev polynomial function refined using 10 parameters. The refinements converged with a χ^2 of 9.70 to 18.08 and R_{wp} of 6.70 to 12.08. The starting structural data was taken from Inorganic Crystal Structure Database (ICSD).[18]

Results and Discussion

The PXRD patterns of the Fe_2As sample (Figure 2) show three noticeable phase transformations in the sample upon heating. The sample composition remains unchanged until about 300 °C, when magnetite, Fe_3O_4 and FeAs are formed. The second phase transformation in the system occurs at around 650 °C, where magnetite transforms into wuestite FeO (Figure 3). It is known that, under low oxygen fugacity, magnetite is more stable than wuestite at lower temperature[19]. The magnetite reaction to produce wuestite probably involves consumption of Fe_2As and further formation of FeAs according to reaction (6):

$$Fe^{2+}Fe_2^{3+}O_4 + Fe_2As \longrightarrow 4\,Fe^{2+}O + FeAs \tag{6}$$

The final transformation takes place at 800 °C, when the known phase of FeAs disappears to be replaced by a phase displaying new unidentified peaks which appear in the PXRD plot (Figure 2). These unidentified peaks disappear upon subsequent cooling below 650 °C, at which point the phase reverts to the familiar structure of FeAs as seen during heating. The peaks were found to belong to a new high-temperature polymorph of FeAs (see below).

Experimental, calculated and difference curves of the final fit for three representative temperature steps for the experiment performed on sample Fe_2As are shown in Figure 3. It should be noted, that formation of very minor amounts of silicate phases (including fayalite)

7
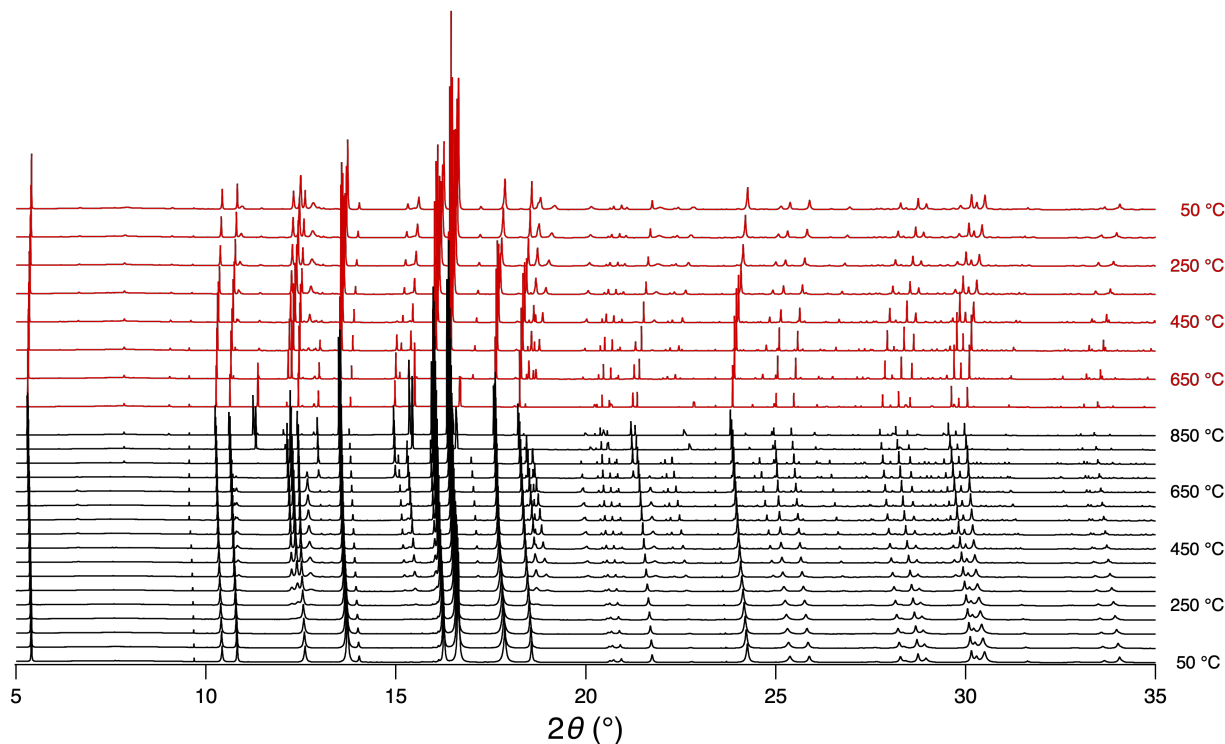
Figure 2: A plot of the PXRD experimental patterns of Fe$_2$As sample upon heating and cooling.

arises during the experiment as a result of chemical reactions between the iron arsenide compound(s) with the silica glass tube walls of the capillary container.

Crystal structure solution of a new high temperature phase of FeAs

At 800 °C the diffraction peaks corresponding to the MnP-type phase of FeAs disappear and some new peaks develop in the pattern. Upon closer analysis, most of these new peaks were in fact triplets and only a few minor ones were single peaks (Figure 4a,b). The single peaks were identified as fayalite. It is known that at low oxygen fugacity wuestite reacts with SiO$_2$ (present as the capillary wall) to form silicates[20].

$$2\,\mathrm{FeO} + \mathrm{SiO_2} \xrightarrow{\text{above 800°C}} \mathrm{Fe_2SiO_4} \tag{7}$$

This distinction was possible because of the excellent data quality. The interpretation is
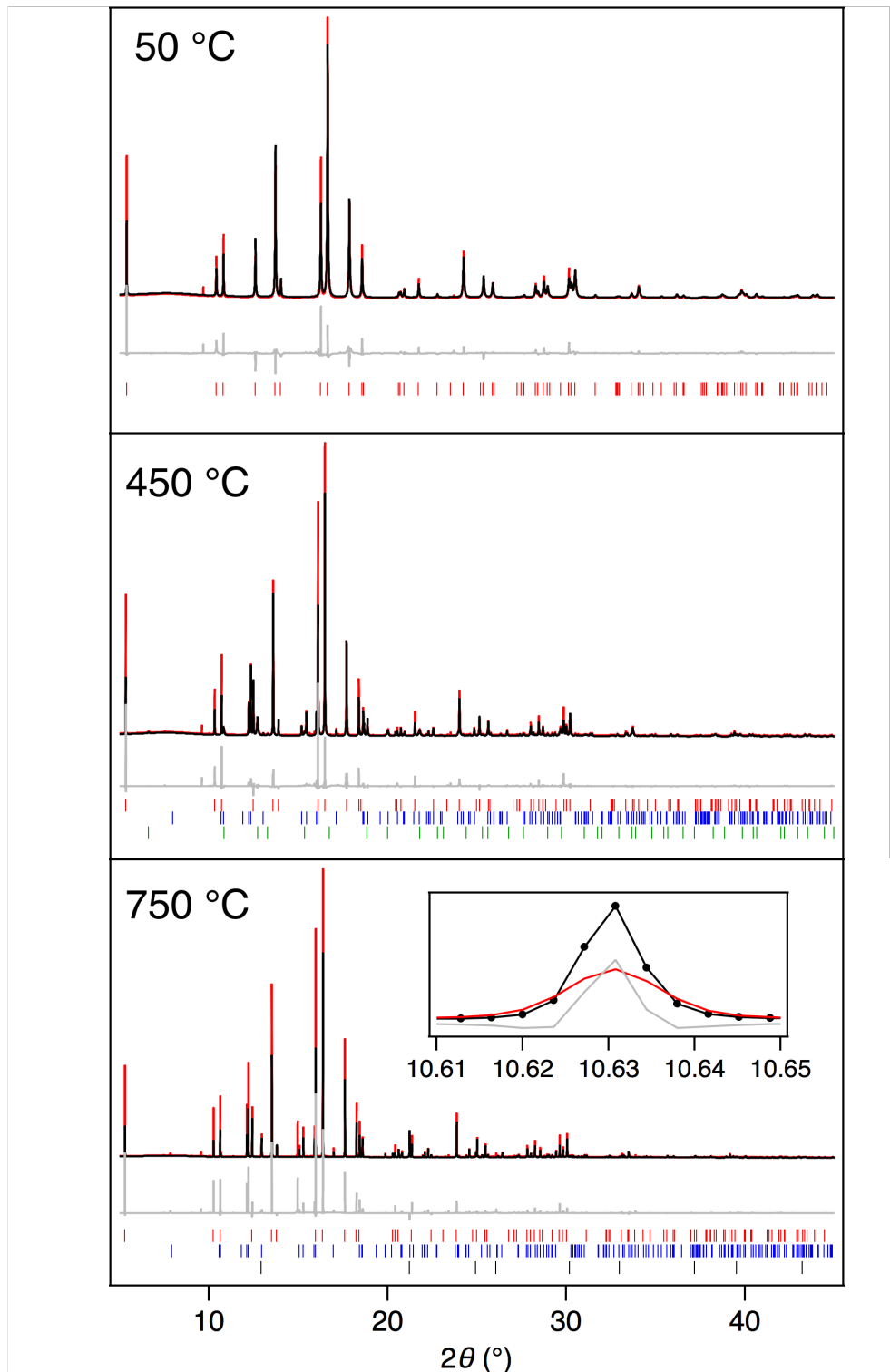
Figure 3: Rietveld refinement of the PXRD patterns of Fe_2As. The experimental (black), calculated (red) and difference (grey) curves are shown. Peak marks: red - Fe_2As, blue - FeAs, green - Fe_3O_4, and black - FeO.

9
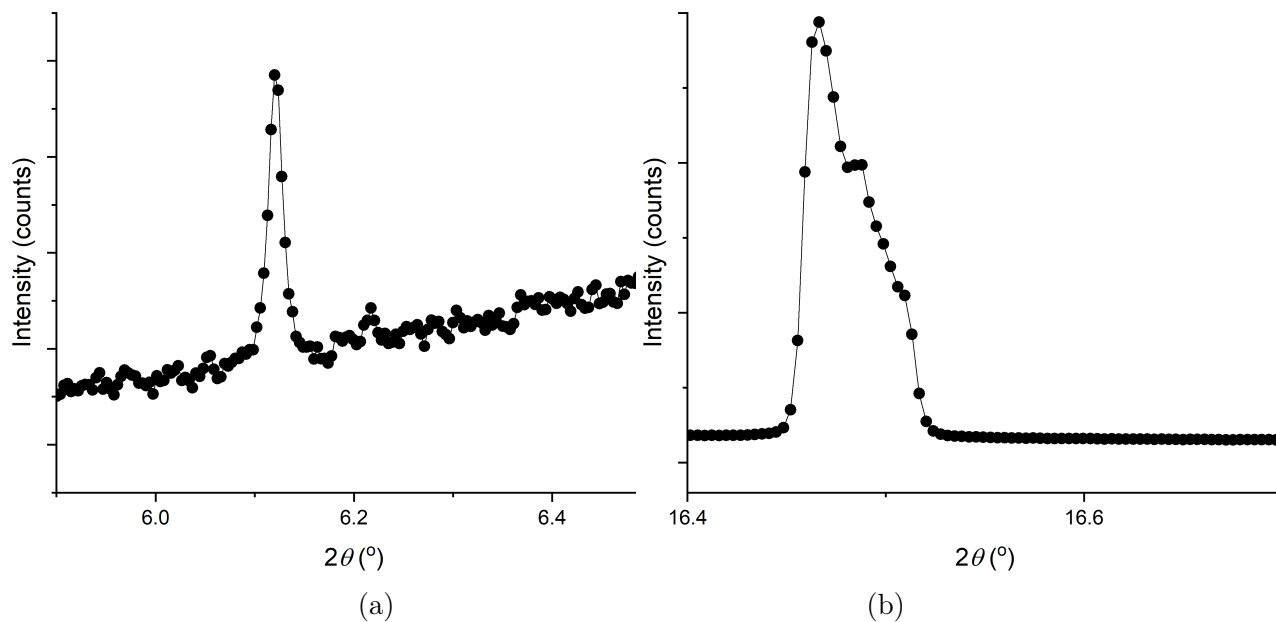
Figure 4: Example of parts of the diffraction patterns of our sample at 800 °C: (a) single peak, (b) triplet peaks.

that a new phase has grown as three individual large single crystals and the triplet reflections were caused by quais-single crystal scattering artefacts: when one or a few bigger crystals are present in the polycrystalline powder in the 0.1 mm thick capillary, their reflections appear to be shifted compared to the expected peak position. Such quasi-single crystal peak intensities are also affected strongly by preferred orientation as their orientation is not randomised. No known iron and/or arsenic compound matches the new triplet peaks, including oxides and silicates.

The triplet peaks were carefully selected, therefore, and fitted using a single pseudo-Voigt peak shape. The peak positions and intensities thus calculated were extracted together with the background to produce a synthetic diffraction pattern (Figure 5). As Figure 6 shows there is virtually no overlap between the triplet peaks and the other peaks in the diffraction pattern. Indexing in cubic, hexagonal, trigonal and tetragonal symmetries was attempted with the indexing algorithm DICVOL[21], which is included in the software DASH[22] from the CCDC suite[23].

Among others, a hexagonal unit cell with a volume of 73 Å^3 gave an excellent Pawley
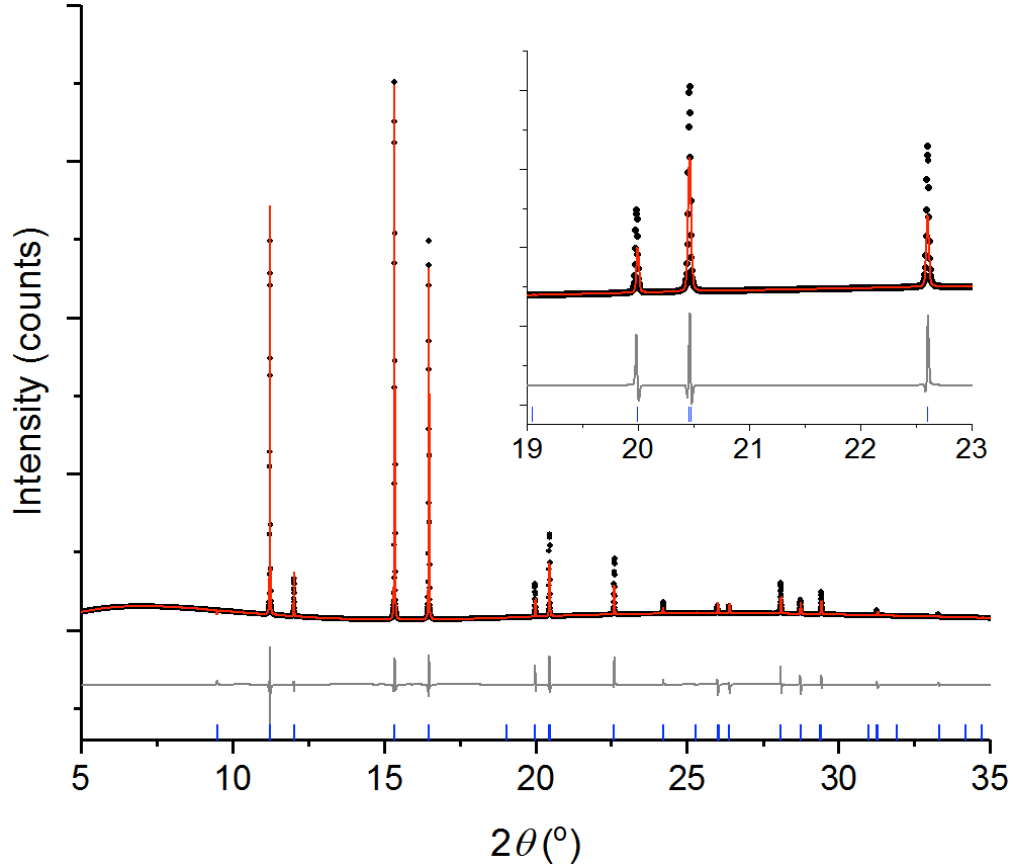
Figure 5: Final Rietveld refinement plot of the high temperature FeAs phase. The observed (black), calculated (red) and difference (grey) patterns, and peak marks for a new phase are shown. The observed pattern has been obtained by fitting the triplet unidentified peaks of the data obtained at 800C with single Pseudo-Voigt peaks.

fit, yielding a and c equal to 3.9439(4) and 5.3897(6) Å, respectively. Space group statistics suggested a 6_3 screw axis along [0 0 1] and a c glide plane along [1 1 0]. A Pawley fit using space group $P6_3/mmc$ - one of the most common space groups in the ICSD database[24] - gave the same χ^2 as for space group $P6$. Before attempting any structure solution trial, we searched in the ICSD database for compounds with cell parameters similar to our refined results to within 3%. Amongst a number of binary compounds with a nickeline (NiAs)-type structure, a CoTe phase (ICSD collection code 53090), isostructural to nickeline (NiAs)[25], was found. Atoms were replaced with Fe and As in the corresponding atomic positions. As can be seen from Figure 5 this structure fitted the experimental data well. The difference curve shows that some of the peaks are slightly shifted (see inset in Figure 5). Rather
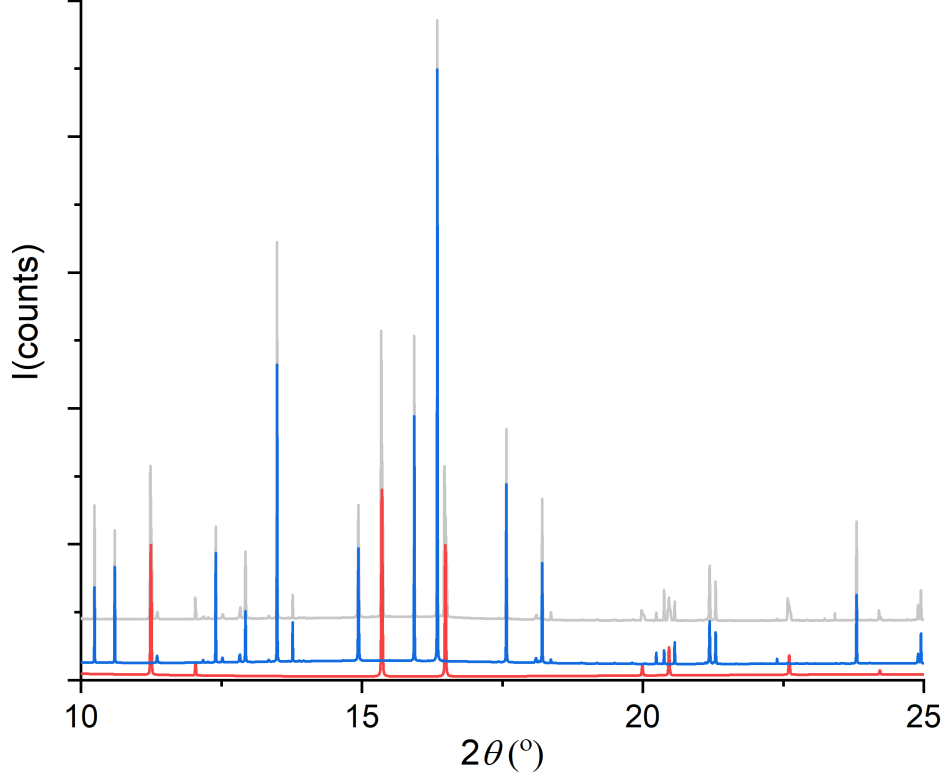
Figure 6: Synthetic pattern (red curve), experimental pattern (grey curve) of Fe_2As at 800 °C, and relative calculated pattern (blue curve) from the Rietveld refinement (including fayalite). Curves have been displaced vertically to aid observation.

than a problem with the cell symmetry and parameters we believe this is due to the way this synthetic pattern was created from an experimental powder pattern affected by single crystal artefacts. Assuming that this high temperature FeAs phase is in fact dominated by three big single crystals, then these crystals would most likely be oriented differently. Misorientation between the crystals also combines with the preferred orientation effect, yielding different intensity ratios for different triplets. This affects the synthetic pattern peak positions giving rise to relatively minor misfit features in the final Rietveld plot (see difference profile of Figure 5 inset). A Rietveld refinement on this synthetic pattern converged with χ^2, R_{wp}, R_{Bragg} equal to 0.86, 5.76%, 3.47%, respectively.

A transition from an MnP-type to a high temperature NiAs-type structure has been observed previously for many transition metal arsenides including TiAs, VAs, CrAs, (Mn,Fe)As, CoAs, NiAs. Heyding and Calvert mentioned the possibility of a phase transition in FeAs

below its melting point. However, they were not able to obtain satisfactory diffraction data, due to attack of the silica capillaries above 900 °C[20]. Selte et al., 1972 did not observe any structure changes in FeAs up to its melting point at 1070±20 °C in their X-ray and neutron diffraction study[9]. However, in their later work, Selte et al., 1973 suggested the possibility of phase transition in FeAs[26]. Although, the existence of this high temperature NiAs-like structure for FeAs was suggested, it has never before been experimentally observed for pure FeAs. Its stability field is indicated by the red portion of the line phase of FeAs shown above in Figure 1.

The two different crystal structures are given in Figure 7 for comparison. It should be noted that the NiAs-type FeAs phase found here is only stable over a very limited temperature range. The variation in phase composition of our sample as a function of temperature is given in Figure 8.
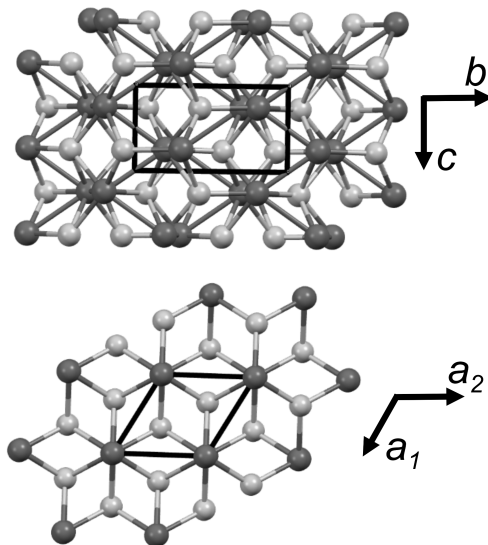

Figure 7: Crystal structures of FeAs phases: MnP-type (top) projected along the a axis and NiAs-type (bottom) projected along the c axis. As atoms and Fe atoms are light grey and dark grey, respectively.

Finally, based on the phase diagram of the Fe-As system given by Okamoto[2], and taking into account experimental conditions (heating up to 850 °C and inert atmosphere) as well as the composition of the sample, the following phases can be identified in the studied
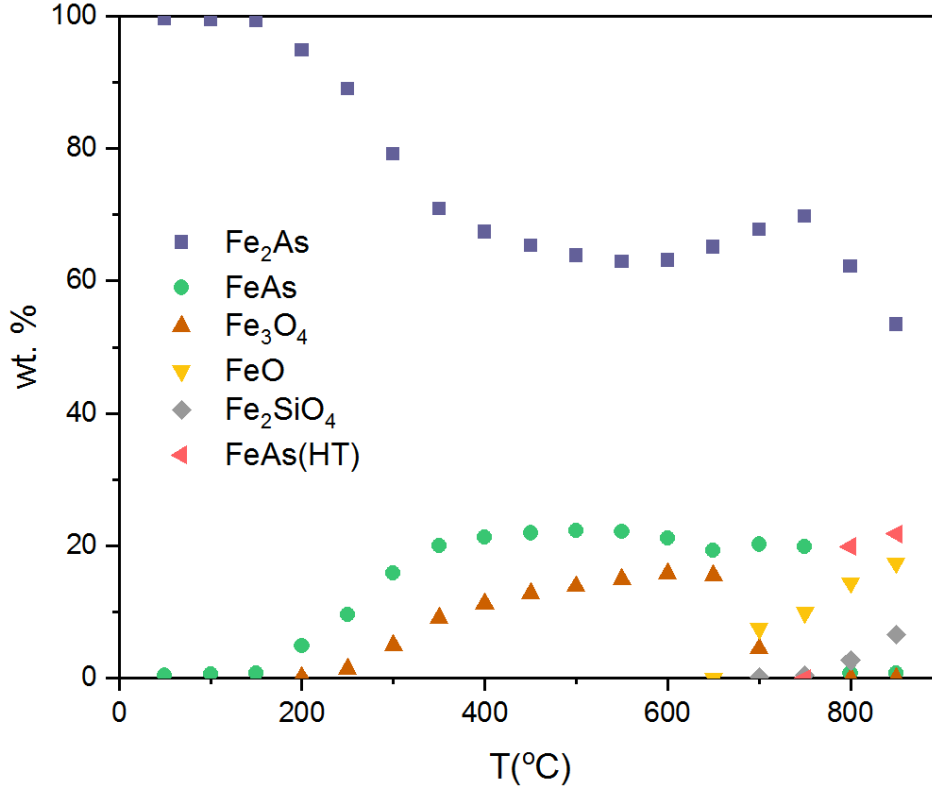
Figure 8: Composition of our sample as a function of temperature as obtained from the Rietveld analysis. The estimated standard deviations were found to be smaller than the symbols.

sample: FeAs, Fe_2As, Fe_3As_2, and $\alpha-Fe$ (Figure 1). However, in this study, we found no evidence for presence of a HT Fe_3As_2 phase. The stability field of Fe_3As_2 has always been considered ambiguous[2]. Existence of Fe_3As_2 below 800°C was initially proposed by Friedrich, 1907[7]. Hagg, 1928 believed that a high-temperature Fe_3As_2 phase was stable only above 795 °C[4]. Heyding and Calvert, 1957 found no indication of the high-temperature Fe_3As_2 phase in iron-arsenic alloys quenched from temperatures above 800°C[20], but did not attempt to do experiments above 795 °C. According to Sawamura and Mori (1954), Fe_3As_2 decomposes eutectoidally at 824 °C[8]. Earlier studies were conducted *ex situ* on heated and quenched or cooled products. This hinders access to intermediate transformation products, therefore could not provide information about full process of phase transformation. Our *in situ* PXRD experiment did not suggest existence of the high-temperature phase Fe_3As_2 at the temperatures from 795 up to 850 °C (Figure 1).

Reference cell parameter data for Fe_2As and FeAs and those obtained in this study are given in Supporting Information (Table S2 and Table S3). The thermal expansion of cell parameters and volume of FeAs with temperature was calculated according to the expression 8 and is in good agreement with data of Selte et al., 1972[9] (Table 2.).

$$\alpha = (L_2 - L_1)/L_0(T_2 - T_1) \tag{8}$$

Table 2: Thermal expansion coefficients of FeAs

Unit cell	α			
	this study		Selte et al., 1972[9]	
a	$14 \times 10^{-6}K^{-1}$	(723 - 1023 K)	$14 \times 10^{-6}K^{-1}$	(775 - 1275 K)
b	$46 \times 10^{-6}K^{-1}$	(523 - 1023 K)	$42 \times 10^{-6}K^{-1}$	(375 - 1075 K)
c	$25 \times 10^{-6}K^{-1}$	(523 - 1023 K)	$23 \times 10^{-6}K^{-1}$	(425 - 1275 K)
V	$100 \times 10^{-6}K^{-1}$	(673 - 1023 K)	$104 \times 10^{-6}K^{-1}$	(975 - 1325 K)

Conclusions

Our temperature-dependent study of a starting diiron arsenide compound allowed ambiguities in the Fe-As binary system to be resolved. For the first time, the existence of a high-temperature FeAs phase with NiAs-type structure has been demonstrated. In addition, no experimental evidence is found for the presence of a high-temperature phase Fe_3As_2. Hence, the phase diagram for the system Fe-As has to be modified accordingly.

Preliminary *in situ* high-temperature PXRD data and identification of various phases upon thermal dissociation of diiron arsenide provide evidence related to phase transformations of iron arsenides upon heating, which is important in defining the thermodynamic state of these materials in real applications.

Acknowledgement

Supporting Information Available

The following files are available as supporting information.

- Photograph of the experimental setup showing the solid-state silicon microstrip detector MYTHEN II (Microstrip sYstem for Time-rEsolved experimeNts).

- The starting structural data of all phases.

- Reference cell parameter data.

- Cell parameters of Fe_2As and FeAs.

References

(1) Seitkan, A.; Redfern, S. Processing double refractory gold-arsenic-bearing concentrates by direct reductive melting. *Minerals Engineering* **2016**, *98*, 286–302.

(2) Okamoto, H. The As-Fe (arsenic-iron) system. *Journal of Phase Equilibria* **1991**, 457–461.

(3) Hagg, G. X-Ray Studies on the System Iron Arsenide (in german). *Zeitschrift für Kristallographie* **1929**, *71*, 134–136.

(4) Hagg, G. X-Ray Studies on the Binary Systems of Iron with Phosphorus, Arsenic, Antimony, and Bismuth (in german). *Zeitschrift für Kristallographie* **1928**, *68*, 470–471.

(5) Buerger, M. The crystal structure of löllingite, *FeAs₂*. *Zeitschrift für Kristallographie - Crystalline Materials* **1932**, 165–187.

(6) Clark, L. The Fe-As-S system – Phase relations and applications. *Economic Geology* **1960**, 1345–1381.

(7) Friedrich, K. Iron and arsenic (in german). *Metallurgie* **1907**, 129–137.

(8) Sawamura, H.; Mori, T. A Supplement to Investigation of Equilibrium Diagram of Fe-As-C System. *Faculty of Engineering of Kyoto University* **1954**, 182–189.

(9) Selte, K.; Kjekshus, A.; Andresen, A. Magnetic structure and properties of FeAs. *Acta Chemica Scandinavica* **1972**, 3101–3113.

(10) Lyman, P.; Prewitt, C. Room-and high-pressure crystal chemistry of CoAs and FeAs. *Acta Crystallographica Section B: Structural Science* **1984**, 14–20.

(11) Strathdee, B.; Pidgeon, L. Thermal decomposition and vapor pressure measurements of arsenopyrite and arsenical ore. *Canadian Mining and Metallurgical Bulletin* **1961**, 883 – 887.

(12) Tkach, M.; Tkachenko, O.; Isakova, L., RA Ugryumova O povedenii arsenidov zheleza pri nagrevanii v vakuume (in rus). Trudy IMiO AN Kaz. SSR. 1977; pp 54–60.

(13) Isabayev, S.; Pashinkin, A.; Mil'ke, E.; Zhambekov, M. *Fiziko-khimicheskiye osnovy sul'fidirovaniya mysh'yaksoderzhashchikh soyedineniy (in rus)*; Alma-Ata: Nauka, 1986.

(14) Khrapunov, V.; Isakova, R.; Spivak, M.; Fedulov, I. Dissotsiatsia diarsenida zheleza (in rus). *Zhurnal Neorganicheskoi Khimii* **1993**, 784–785.

(15) Khrapunov, V.; Spivak, M.; Spitsyn, V.; Khlystov, A.; Isakova, R.; Fedulov, I. O termicheskom povedenii arsenopirita (in rus). *Zhurnal Neorganicheskoi Khimii* **1991**, 2786 – 2790.

(16) Willmott, P.; Meister, D.; Leake, S.; Lange, M.; Bergamaschi, A.; Böge, M.; Calvi, M.; Cancellieri, C.; Casati, N.; Cervellino, A. The materials science beamline upgrade at the Swiss Light Source. *Journal of Synchrotron Radiation* **2013**, 667–682.

(17) Coelho, A. TOPAS-Academic. Coelho Software, Brisbane, Australia, 2007.

(18) Inorganic Crystal Structure Database (2015). `http://icsd.cds.rsc.org/search/basic.xhtml`, Available from: http://icsd.cds.rsc.org/search/basic.xhtml. Accessed 15 September 2015.

(19) Lindsley, D. Experimental studies of oxide minerals. *Reviews in Mineralogy and Geochemistry* **1991**, 69–106.

(20) Heyding, R.; Calvert, L. Arsenides of Transition Metals: The Arsenides of Iron and Cobalt. *Canadian Journal of Chemistry* **1957**, 449–457.

(21) Boultif, A.; Louër, D. Powder pattern indexing with the dichotomy method. *Journal of Applied Crystallography* **2004**, 724–731.

(22) David, W. I.; Shankland, K.; van de Streek, J.; Pidcock, E.; Motherwell, W. S.; Cole, J. C. DASH: a program for crystal structure determination from powder diffraction data. *Journal of Applied Crystallography* **2006**, *39*, 910–915.

(23) Groom, C. R.; Bruno, I. J.; Lightfoot, M. P.; Ward, S. C. The Cambridge structural database. *Acta Crystallographica Section B: Structural Science, Crystal Engineering and Materials* **2016**, 171–179.

(24) Urusov, V.; Nadezhina, T. Frequency distribution and selection of space groups in inorganic crystal chemistry. *Journal of Structural Chemistry* **2009**, *50*, 22–37.

(25) de Meester de Betzembroeck, P.; Naud, J. Étude par Diffraction-X de Quelques Composés du Système Ni-Co-Te Obtenus par Synthèse Thermique. *Bulletin des Sociétés Chimiques Belges* **1971**, 107–116.

(26) Selte, K.; Kjekshus, A. Phase Transitions Between the MnP and NiAs Type Structures. *Acta Chemica Scandinavica* **1973**, 3195–3206.

For Table of Contents Only
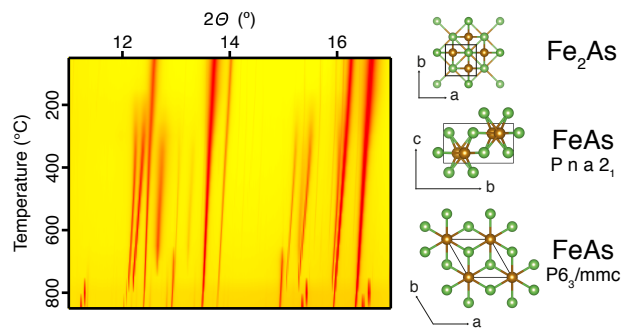
Figure 9: For Table of Contents Only.

Synopsis